Res Chem Intermed
DOI 10.1007/s11164-013-1122-3

Corrosion inhibition investigations of 3-acetylpyridine semicarbazone on carbon steel in hydrochloric acid medium

Vinod P. Raphael · K. Joby Thomas · K. S. Shaju · Aby Paul

Received: 10 November 2012 / Accepted: 14 February 2013

Abstract The corrosion inhibition efficiency of 3-acetylpyridine-semicarbazide (3APSC) on carbon steel (CS) in 1.0 M HCl solution has been investigated using weight loss measurements, electrochemical impedance spectroscopy (EIS) and potentiodynamic polarization studies. The results show that inhibition efficiency on metal increases with the inhibitor concentration. 3APSC exhibited marked inhibition towards carbon steel in HCl medium even at low concentrations. The adsorption of inhibitor on the surfaces of the corroding metal obeys the Langmiur isotherm and thermodynamic parameters (K_{ads}, ΔG^0_{ads}) were calculated. Activation parameters of the corrosion process (E_a, ΔH^* and ΔS^*) were also calculated from the corrosion rates. Polarization studies revealed that 3APSC act as a mixed-type inhibitor. Surface analysis of the metal specimens was performed by scanning electron microscopy.

Keywords Carbon steel · Semicarbazone · Corrosion inhibitors · Isotherm · SEM

Introduction

Research on carbon steel (CS) corrosion is of great importance in the field of metal industries. Techniques such as picking, de-scaling, etc., are usually employed for the cleaning of the metal surfaces which would require enormous amounts of hydrochloric acid. This surface cleaning process will escalate the metallic dissolution and it is considered as a major reason for the corrosion problems in the world. Many organic molecules containing hetero atoms [1–3] and compounds

V. P. Raphael · K. J. Thomas (✉) · K. S. Shaju · A. Paul
Research Division, Department of Chemistry, St.Thomas' College (University of Calicut), Thrissur, Kerala, India
e-mail: drjobythomask@gmail.com

Published online: 01 March 2013

containing azomethine linkage (C=N) have been reported to act as good corrosion inhibitors for CS, aluminum, copper and zinc in acidic media [4–11].

Various researchers during the past decade have been actively probing into the field of corrosion in search of novel corrosion inhibitors and exploring the mechanism of inhibition, mainly through electrochemical investigations [8, 9]. A literature survey revealed that no work has been reported for the corrosion inhibition of compounds derived from 3-acetylpyridine in acid media. The present investigation was undertaken to examine the corrosion inhibition capacity and the mechanism of inhibition of a heterocyclic semicarbazone (3APSC) derived from 3-acetylpyridine and semicarbazide in 1 M HCl solution on carbon steel. The study was performed by weight loss measurements, electrochemical impedance spectroscopy (EIS) and potentiodynamic polarization analysis.

Experimental

Inhibitor

Heterocyclic semicarbazone was obtained by the condensation of an equimolar mixture of 3-acetylpyridine and semicarbazide in ethanol medium. The reaction mixture was refluxed for 2 h, evaporated and cooled in an ice bath to obtain a white-coloured compound. Figure 1 shows the molecular structure of heterocyclic semicarbazone 3APSC. Anal.calcd. for $C_8H_{10}N_4O_1$: C, 53.93; H, 5.61; N, 31.46 %. Found C, 53.65; H, 5.99; N, 31.81; m.p. = 199 °C; IR (KBr): $\nu_{C=N} = 1{,}601\ cm^{-1}$ Mass: M^+ peak m/z: 178.

Solutions

The aggressive solutions of 1 M HCl were prepared by dilution of AR grade 37 % of HCl (Merck) with deionized water. Inhibitor solutions were prepared in the range 0.2–1 mM concentrations.

Gravimetric studies

Carbon steel specimens of chemical composition C, 0.58 %; Mn, 0.07 %; P, 0.02 %; S, 0.015 %; Si, 0.02 % and the rest Fe, dimensions 1.0 × 1.0 × 0.1 cm, were cut and abraded by a series of silicon carbide papers (grades 200, 400, 600, 800, 1,000, 1,200, and 2,000). The exact area and thickness of each specimen were measured and washed with distilled water containing detergent. Specimens were then degreased with acetone and finally dried. After weighing, specimens

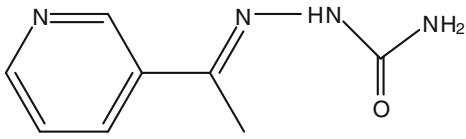

Fig. 1 Molecular structure of 3APSC

were immersed in 50 ml acid solutions in a water bath at 30–60 °C in the absence and presence of the inhibitor 3APSC, using hooks and fishing lines. Weight loss of metal specimens was noted after 24 h. The experiments were carried out in duplicate and the average values were reported. The corrosion rate (v) is calculated by the following equation [8].

$$v = \frac{W}{St} \tag{1}$$

where W is the average weight loss of coupon, S is the total area of specimens, and t is the time of treatment. The percentage of inhibition efficiency (η) is defined by [12].

$$\eta_w\% = \frac{v_0 - v}{v_0} \times 100 \tag{2}$$

where v_0 and v are the corrosion rates of uninhibited and inhibited specimens, respectively.

AC impedance study

The impedance experiments were conducted using the Ivium compactstat-e electrochemical system. In the three-electrode assembly, saturated calomel electrode (SCE) was used as the reference electrode. A platinum electrode having and area of 1 cm^2 was taken as the counter electrode. Metal specimens with an exposed area of 1 cm^2 were used as the working electrode, while 1 M HCl solution was taken as the electrolyte. The working areas of the metal specimens were exposed to the electrolyte for 1 h prior to the measurement. All tests were performed under unstirred conditions. Constant potential (OCP) was maintained in all measurements and a frequency range of 1 kHz–100 MHz with amplitude of 10 mV as excitation signal was employed. The percentage of inhibitions from impedance measurements were calculated using charge transfer resistance values by the following expression [2]:

$$\eta_{\mathrm{EIS}}\% = \frac{R_{\mathrm{ct}} - R_{\mathrm{ct}}^{'}}{R_{\mathrm{ct}}} \times 100 \tag{3}$$

where R_{ct} and R_{ct}' are the charge transfer resistances of working electrode with and without inhibitor, respectively.

Polarization studies

Electrochemical polarization studies of CS specimens in 1 M HCl with and without inhibitor were performed by recording anodic and cathodic potentiodynamic polarization curves. Polarization plots were obtained in the electrode potential range −100 to +100 mV versus equilibrium potential at a sweep rate of 1 mV s^{-1}. Tafel polarization analyses were done by extrapolating anodic and cathodic curves to the potential axis to obtain corrosion current densities (I_{corr}). The percentage of

inhibition efficiency (η_{pol} %) was evaluated from the measured I_{corr} values using the following relationship [13]:

$$\eta_{pol}\% = \frac{I_{corr} - I'_{corr}}{I_{corr}} \times 100 \quad (4)$$

where I_{corr} and I_{corr}' are the corrosion current densities of the exposed area of the working electrode in the absence and presence of the inhibitor.

From the slope analysis of the linear polarization curves in the vicinity of the corrosion potential of blank and different concentrations of the inhibitor, the values of polarization resistance (R_p) in 1 M HCl solution were obtained. From the evaluated polarization resistance, the inhibition efficiency was calculated using the relationship

$$\eta_{R_p}\% = \frac{R'_p - R_p}{R'_p} \times 100 \quad (5)$$

where R_p' and R_p are the polarization resistance in the presence and absence of inhibitor, respectively [2].

Scanning electron microscopy

Surface analyses were performed using a scanning electron microscope (model Hitachi SU6600). SEM images were obtained from the CS surface after the immersion in 1 M HCl solutions in the absence and presence of the inhibitor 3APSC (1 mM) for 24 h at 30 °C.

Results and discussion

Gravimetric corrosion inhibition studies

The corrosion rates of CS specimens and inhibition efficiencies for a period of 24 h are listed in Table 1. The corrosion rates markedly decreased with the inhibitor concentration. This can be attributed to the increasing surface coverage of the inhibitor molecules on the metal through adsorption with the increase in concentration [14]. Even at a low concentration of 0.2 mM, 3APSC molecules exhibited 60 % inhibition efficiency on carbon steel at 30 °C. From 0.2 to 0.8 mM inhibitor concentration, the percentage of inhibition efficiencies showed a marked increase. Beyond 0.8 mM, η_W % got a saturation character and did not change noticeably (critical inhibitor concentration) [15, 16].

Comparison of inhibition efficiency of 3APSC with semicarbazide

To compare the inhibition efficiencies of 3APSC and the parent amine semicarbazide, weight loss measurements of CS specimens were performed in 1 M HCl at 30 °C. The percentage of corrosion inhibition efficiencies obtained for 3APSC and

Table 1 The corrosion rate and percentage of inhibition efficiency for CS specimens immersed in 1 M HCl at 30 °C for 24 h in the presence and absence of 3APSC

C (mM)	Corrosion rate (mm y^{-1})	Inhibition efficiency (η_W %)
0	6.54	–
0.2	2.60	60.33
0.4	1.91	70.77
0.6	1.15	82.40
0.8	0.933	85.73
1.0	0.932	85.75

Table 2 Comparison of percentage of inhibition efficiencies of 3APSC and semicarbazide

C (mM))	Semicarbazide (η_W %)	3APSC (η_W %)
0.2	60.23	60.33
0.6	57.63	82.40
1.0	45.65	85.75

semicarbazide are listed in Table 2. The inhibition efficiency of the 3APSC was significantly higher than that of semicarbazide for the studied concentrations. The η_W % of semicarbazide decreased considerably with concentration, but the opposite trend was exhibited by 3APSC. This investigation clearly establishes the role of azomethine linkage (C=N) present in the 3APSC which actively participate in the corrosion inhibition mechanism.

Adsorption isotherm and free energy of adsorption

The mechanism of adsorption and the surface behavior of organic molecules can be easily viewed through adsorption isotherms. Different models of adsorption isotherms considered are the Langmiur, Temkin, Frumkin and Freundlich isotherms. For the evaluation of thermodynamic parameters, it is necessary to determine the best fit isotherm with the aid of the correlation coefficient (R^2). Among the isotherms mentioned above, the best description of the adsorption behavior of 3APSC on CS specimens in 1 M HCl was the Langmiur adsorption isotherm which can be expressed as

$$\frac{C}{\theta} = \frac{1}{K_{ads}} + C \tag{6}$$

where C is the concentration of the inhibitor, θ is the fractional surface coverage and K_{ads} is the adsorption equilibrium constant [17]. Figure 2 represents the adsorption plot of 3APSC obtained by the weight loss measurements of CS specimens in 1 M HCl at 30 °C.

The adsorption equilibrium constant K_{ads} is related to the standard free energy of adsorption ΔG^0_{ads}, by

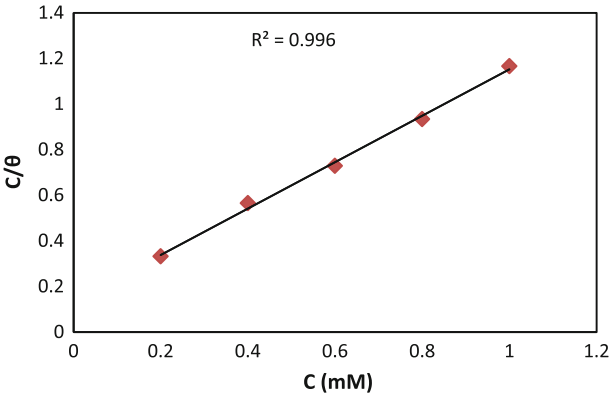

Fig. 2 Langmiur adsorption isotherm for adsorption of 3APSC on CS surface in 1 M HCl at 30 °C

$$\Delta G^0_{\text{ads}} = -RT \ln(55.5\, K_{\text{ads}}) \tag{7}$$

where 55.5 is the molar concentration of water, R is the universal gas constant and T is the temperature in K [18]. ΔG^0_{ads} for 3APSC on CS showed negative values indicating the spontaneity of the process. The value of ΔG^0_{ads} up to -20 kJ mol^{-1} is an indication of the electrostatic interaction of the charged molecule and the charged surface of the metal (physisorption) while ΔG^0_{ads} is more negative than -40 kJ implies that inhibitor molecules are adsorbed strongly on the metal surface through a co-ordinate type bond (chemisorption) [18–20]. In the present investigation, $K_{\text{ads}} = 7{,}519$ and $\Delta G^0_{\text{ads}} = -33.4$ kJ mol^{-1} suggesting that the adsorption of inhibitor involves both electrostatic adsorption and chemisorption.

Effect of temperature

The effect of temperature on corrosion was also evaluated using weight loss measurement in the temperature range of 30–60 °C. The activation energy of corrosion with and without the inhibitor could be calculated by the Arrhenius equation

$$K = A \exp\left(-\frac{E_{\text{a}}}{RT}\right) \tag{8}$$

where K is the rate of corrosion, E_{a} the activation energy, A the frequency factor, T the temperature in Kelvin scale, and R is the gas constant. Linear plots between logK and 1,000/T (Fig. 3) having regression coefficients close to unity indicate that the corrosion of CS in HCl could be explained by the simple kinetic model. Enthalpy and entropy of activation (ΔH^*, ΔS^*) were calculated from the transition state theory [21]

$$K = \left(\frac{RT}{Nh}\right)\left(\frac{\Delta S*}{R}\right) \exp\left(\frac{-\Delta H*}{RT}\right) \tag{9}$$

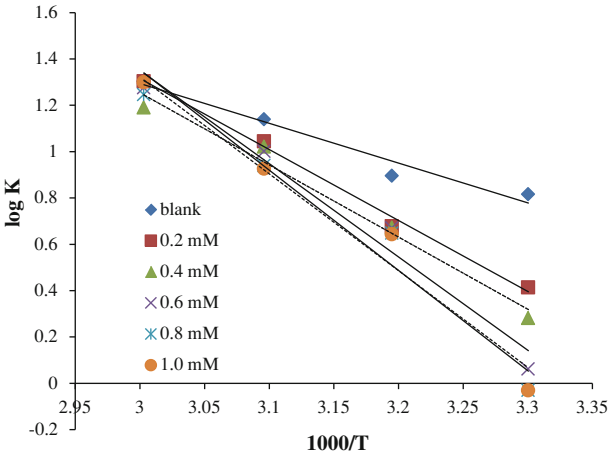

Fig. 3 Arrhenius plots to calculate the activation energy of corrosion of CS in the absence and presence of 3APSC

where N is the Avogadros number and h is the Planks constant. A plot of $\log(K/T)$ versus $1/T$ gave straight lines for the corrosion of CS in 1 M HCl in the presence and absence of the inhibitor (Fig. 4). Table 3 explores the activation energy and thermodynamic parameters of corrosion of CS in 1 M HCl with and without the inhibitor 3APSC. Activation energy of dissolution of the metal increased with the inhibitor concentration. This implies that the reluctance of dissolution of metal was increased with the inhibitor concentration. Positive signs of enthalpies with a regular rise reflect the endothermic nature of dissolution and the increasing difficulty of corrosion with the inhibitor. It is evident from Table 3 that the entropy of activation increases with the inhibitor concentration. For the blank and low concentrations of the inhibitor, the entropy of activation is large and negative. This implies that in the rate determining step, a decrease in disordering takes place on going from reactants to the activated complex and the activated molecules were in higher order state than that at the initial state. But as the concentration of inhibitor rises, the disordering of activated complex rises and the entropy of activation acquires positive values.

Surface analysis using SEM

SEM images of CS surfaces are given in Fig. 5a–c. On close inspection and comparison of Fig. 5a, b, it is evident that the surface of CS was severely corroded in the acidic solution. Small pits and mild cracks on the bare metal surface were due to the irregularity of the metal surface and the effect of surface polishing. These polishing lines and cracks were absent on the surface of the metal in HCl in the absence of the inhibitor. Figure 5c represents the surface image of the metal in the presence of the inhibitor (1 mM). Comparison of the textures of images in Fig. 5b, c revealed that less damage on the surface of CS happened in the presence of the inhibitor 3APSC. This implies that the corrosion was suppressed by the formation of a good protective film of 3APSC through adsorption.

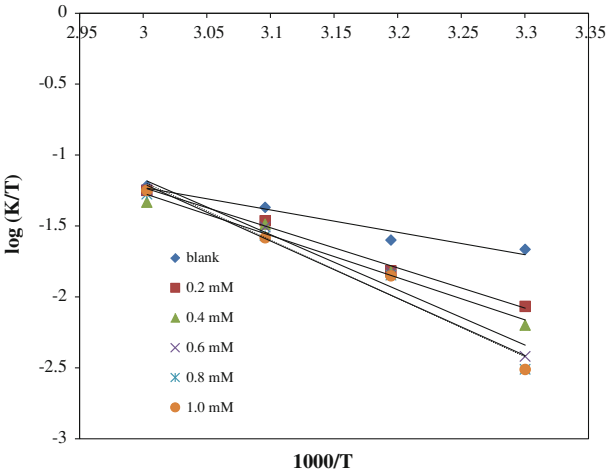

Fig. 4 Plots of log(K/T) versus 1,000/T for the corrosion of CS in the absence and presence of 3APSC

Table 3 Thermodynamic parameters of corrosion of CS in 1 M HCl with and without the inhibitor 3APSC

C (mM)	E_a (kJ mol^{-1})	A	ΔH^* (kJ mol^{-1})	ΔS^* (J mol^{-1} K^{-1})
Blank	32.86	2.76×10^{6}	30.21	−100.88
0.2	58.59	3.09×0^{10}	54.19	−20.26
0.4	59.62	3.89×10^{10}	56.98	−12.62
0.6	77.12	2.69×10^{13}	74.48	41.76
0.8	79.96	7.08×10^{13}	77.32	49.61
1.0	82.87	2.13×10^{14}	78.68	54.02

Impedance studies

The corrosion response of CS in 1 M HCl in the presence and absence of inhibitor has been investigated using AC impedance measurements at 30 °C. Figure 6a, b represents the Nyquist plots and Bode plots, respectively, for CS specimens 1 M HCl. It is evident from the plots that the impedance response of metal specimens showed a marked difference in the presence and absence of the inhibitor 3APSC. The semicircles showed slight irregularities which may be attributed to the roughness or the non-homogeneous nature of the metal surface [22–25].

Impedance behavior can be well explained by pure electric models that can verify and enable the calculation of numerical values corresponding to the physical and chemical properties of the electrochemical system under examination [26]. The simple equivalent circuit that fits many electrochemical systems is composed of a double-layer capacitance, R_s and R_{ct} [5, 27, 30]. To reduce the effects due to surface irregularities of the metal, a constant phase element (CPE) is introduced into the circuit instead of a pure double-layer capacitance which gives a more accurate fit as shown in Fig. 7 [28, 29].

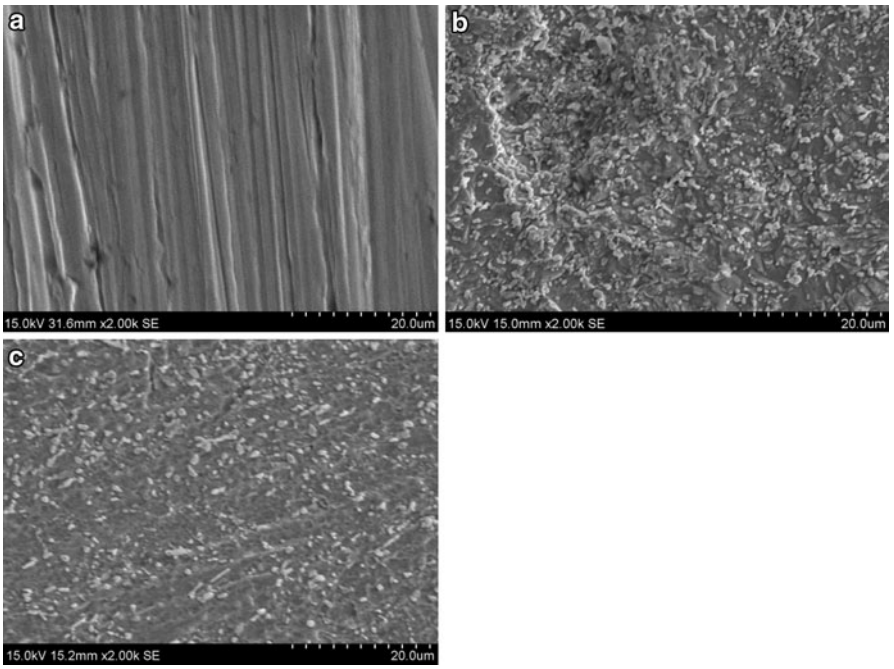

Fig. 5 **a** SEM image of bare CS surface. **b** SEM image of CS surface in 1 M HCl (blank). **c** SEM image of CS surface in 1M HCl and inhibitor (1 mM)

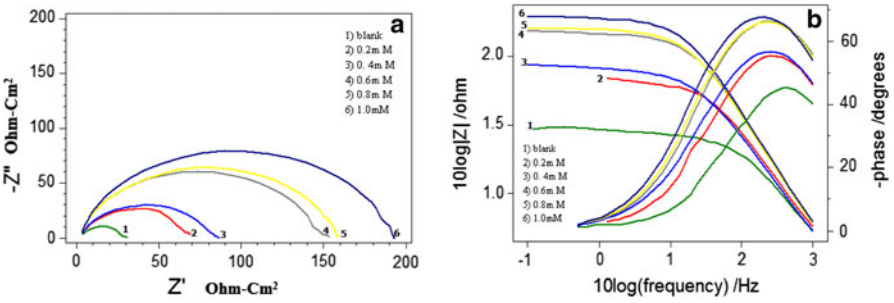

Fig. 6 **a** Nyquist plots **b** Bode plots for CS specimens in 1 M HCl for blank and varying concentration of inhibitor

$$\text{The impedance of CPE can be expressed as } Z_{\text{CPE}} = \frac{1}{Y_0(j\omega)^n} \tag{10}$$

where Y_0 is the magnitude of CPE, n is the exponent (phase shift), ω is the angular frequency and j is the imaginary unit. CPE may be resistance, capacitance and inductance depending upon the values of n [5]. In all experiments, the observed value of n ranges between 0.75 and 1.0, suggesting the capacitive response of CPE.

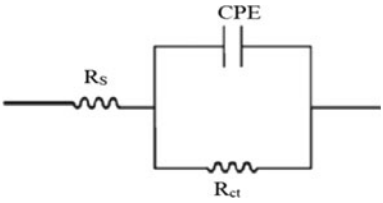

Fig. 7 Equivalent circuit fitting for EIS measurements

Table 4 Electrochemical Impedance parameters of CS specimens in 1 M HCl at 30 °C in the absence and presence of 3APSC

C (mM)	R_{ct} (Ωcm^2)	C_{dl} ($\mu F\ cm^{-2}$)	η_{EIS} %
0	23.08	76.36	–
0.2	58.32	63.87	60.43
0.4	72.17	81.59	68.02
0.6	136.1	51.06	83.04
0.8	144.7	54.18	84.05
1.0	177.3	50.98	86.98

The EIS parameters such as R_{ct}, R_s and CPE and the calculated values of percentage of inhibition (η_{EIS} %) of CS specimens are listed in Table 4.

From Table 4, it is clear that R_{ct} values are increased with increasing inhibitor concentration. The value of R_{ct} is a measure of electron transfer across the exposed area of the metal surface and is inversely proportional to the rate of corrosion [25]. The decrease in capacitance values C_{dl} with inhibitor concentration can be attributed to the decrease in local dielectric constant and/or increase in the thickness of the electrical double layer. This emphasizes the action of the inhibitor molecules by adsorption at the metal–solution interface [30]. The percentage of inhibitions (η_{EIS} %) showed a regular increase with increase in inhibitor concentration. A maximum of 87 % inhibition efficiency could be achieved at an inhibitor concentration of 1 mM.

Potentiodynamic polarization studies

Potentiodynamic polarization curves for CS specimens in the presence and absence of 3APSC in 1 M HCl is shown in Fig. 8.

Polarization parameters like corrosion current densities (I_{corr}), corrosion potential (E_{corr}), cathodic Tafel slope (b_c), anodic Tafel slope (b_a), and inhibition efficiency (E_p) for CS specimens are listed in Table 5. A prominent decrease in the corrosion current density (I_{corr}) was observed in the presence of inhibitor 3APSC. A lowest value of I_{corr} was noticed for the inhibitor solution of concentration 1 mM which exhibited a maximum inhibition efficiency of 87 %. Since the value of b_c and b_a changed in the presence of 3APSC, it may be assumed that the inhibitor molecules are uniformly adsorbed on cathodic and cathodic sites. Generally, if the shift of E_{corr} is >85 with respect to E_{corr} of the uninhibited solution, the inhibitor can be viewed as of cathodic or anodic type [20, 31, 32]. In the present study, the maximum shift of E_{corr} is 28 mV, suggesting that 3APSC acts as a mixed-type inhibitor for CS specimens in 1 MHCl.

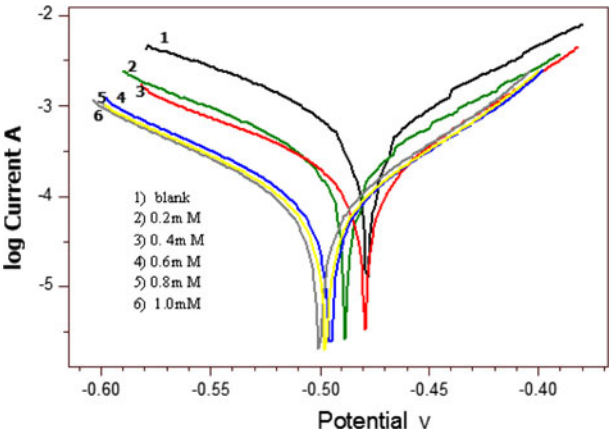

Fig. 8 Tafel plots of CS specimens in 1 M HCl at 30 °C, with and without inhibitor 3APSC

Mechanism of inhibition

It is well known that the surface of the metal is positively charged in acidic media [33]. It is believed that the Cl^- ions could be specifically adsorbed on the metal surface and create an excess of negative charge on the surface. This will favor the adsorption of protonated semicarbazone ($3APSCH^+$) on the surface and hence reduce the dissolution of Fe to Fe^{2+} [34]. Besides this electrostatic interaction between the protonated semicarbazone and the metal surface, other possible interactions are (1) interaction of unshared electron pairs in the molecule with the metal, (2) interaction of π-electrons with the metal, and (3) a combination of types (1 and 2) [35, 36]. If one examines the structure of semicarbazone (3APSC), many potential sources of inhibitor–metal interaction can be recognized. The unshared pair of electrons present on *N* atoms is of key importance in making the coordinate

Table 5 Potentiodynamic polarization parameters of CS specimens in 1 M HCl at 30 °C in the absence and presence of 3APSC

Tafel data						Linear polarization data	
C (mM)	E_{corr} (mV SCE^{-1})	I_{corr} (μA cm^{-2})	b_c (mV dec^{-1})	b_a (mV dec^{-1})	η_{pol} %	$R_p(\Omega)$	η_{Rp} %
0	−474	499.6	102	77	–	38.14	–
0.2	−484	207.4	101	74	58.49	89.54	57.40
0.4	−476	150.2	106	65	69.94	117.2	67.46
0.6	−492	71.13	89	65	85.76	230.6	83.32
0.8	−498	66.88	88	64	86.61	241.1	84.18
1.0	−495	65.99	88	64	86.79	244.3	84.39

bond with the metal. The π-electron cloud of the aromatic rings and the azomethine linkage also participates in the inhibition mechanism. Furthermore, the double bonds in the inhibitor molecule permit the back donation of metal *d* electrons to the π*-orbital, and this type of interaction cannot occur with amines [37]. This can be justified by the lower inhibition efficiency of the semicarbazide than that of semicarbazone.

Conclusions

1. 3APSC is a good inhibitor for CS in 1 M HCl. A maximum of 87 % of inhibition efficiency could be achieved with this inhibitor by Tafel polarization studies.
2. Compared to the parent amine semicarbazide, 3APSC exhibited higher inhibition efficiencies.
3. The inhibition mechanism is explained by adsorption. Adsorption of 3APSC on CS surface obey the Langmiur adsorption isotherm.
4. The thermodynamic parameters of the adsorption are calculated from the adsorption isotherms which showed that both physisorption and chemisorption are involved in the inhibition process.

References

1. F. Bentiss, M. Traisnel, L. Gengembre, M. Lagrenée, Appl. Surf. Sci. **161**, 194 (2000)
2. A. Raman, P. Labine, Reviews on corrosion inhibitor science and technology, vol. 1 (NACE, Houston, TX, 1986), p.20
3. E.E. Oguzie, Mater. Lett. **59**, 1076 (2005)
4. A. Yurt, O. Aykın, Corros. Sci. **53**, 3725 (2011)
5. A.K. Singh, S.K. Shukla, M. Singh, M.A. Quraishi, Mater. Chem. Phy. **129**, 68 (2011)
6. M. Behpour, S.M. Ghoreishi, N. Soltani, M. Salavati-Niasari, M. Hamadanian, A. Gandomi, Corros. Sci. **50**, 2172 (2008)
7. K.S. Jacob, G. Parameswaran, Corros. Sci. **52**, 224 (2010)
8. S. Deng, X. Li, H. Fu, Corros. Sci. **53**, 3596 (2011)
9. X. Li, S. Deng, H. Fu, Mater. Chem. Phy. **129**, 696 (2011)
10. A. Bansiwal, P. Anthony, S.P. Mathur, Br. Corros. J. **35**(4), 301 (2000)
11. S. Li, S. Chen, S. Lei, H. Ma, R. Yu, D. Liu, Corros. Sci. **41**, 1273 (1999)
12. AST G-31-72, Standard recommended practice for the laboratory immersion corrosion testing of metals, ASTM, Philadelphia, 1990
13. H.A. Sorkhabi, B. Shaabani, D. Seifzadeh, Electrochim. Acta **50**, 3446 (2005)
14. I.B. Obot, N.O. Obi-Egbedi, Corros. Sci. **52**, 198 (2010)
15. M.A. Quraishi, D. Jamal, M. Luqman, Indian J. Chem. Technol. **9**, 497 (2002)
16. K.C. Emregül, O. Atakol, Mater. Chem. Phys. **83**, 373 (2004)
17. X. Li, S. Deng, H. Fu, T. Li, Electrochim. Acta **54**, 4089 (2009)
18. E. Cano, J.L. Polo, A. La Iglesia, J.M. Bastidas, Adsorption **10**, 219 (2004)
19. F. Bentiss, M. Lebrini, M. Lagrenée, Corros. Sci. **47**, 2915 (2005)
20. W. Li, Q. He, S. Zhang, C. Pei, B. Hou, J. Appl. Electrochem. **38**, 289 (2008)
21. M. Bouklah, N. Benchat, B. Hammouti, A. Aouniti, S. Kertit, Mater. Lett. **60**, 1901 (2006)
22. H.H. Hassan, E. Abdelghani, M.A. Amin, Electrochim. Acta **52**, 6359 (2007)
23. M.S. Abdel-Aal, M.S. Morad, Br. Corros. J. **36**, 253 (2001)

24. P. Bommersbach, C.A. Dumont, J.P. Millet, B. Normand, Electrochim. Acta **51**, 1076 (2005)
25. F. Mansfeld, Corrosion **36**, 301 (1981)
26. A.S. Priya, V.S. Muralidharam, A. Subramannia, Corrosion **64**, 541 (2008)
27. M. El Azhar, B. Mernari, M. Traisnel, F. Bentiss, M. Lagrenée, Corros. Sci. **43**, 2229 (2001)
28. A. Yurt, A. Balaban, S.U. Kandemir, G. Bereket, B. Erk, Mater. Chem. Phys. **85**, 420 (2004)
29. J.R. Macdonald, W.B. Johnson, J.R. Macdonald (eds.), *Theory in impedance spectroscopy* (Wiley, New York, 1987)
30. M. MaCafferty, N. Hackerman, J. Electrochim. Soc. **119**, 146 (1972)
31. X. Li, S. Deng, H. Fu, Corros. Sci. **51**, 1344 (2009)
32. E.S. Ferreira, C. Giacomelli, F.C. Giacomelli, A. Spinelli, Mater. Chem. Phys. **83**, 129 (2004)
33. Q. Qu, Z. Hao, S. Jiang, L. Li, W. Bai, Mater. Corros. **59**, 883 (2008)
34. F. Bentiss, M. Traisnel, M. Lagrenee, Corros. Sci. **42**, 127 (2000)
35. D.P. Schweinsberg, G.A. George, A.K. Nanayakkara, D.A. Steinert, Corros. Sci. **30**, 33 (1988)
36. H. Shokry, M. Yuasa, I. Sekine, R.M. Issa, H.Y. El-baradie, G.K. Gomma, Corros. Sci. **40**, 2173 (1998)
37. A.K. Singh, M.A. Quraishi, J. Appl. Electrochem. **40**, 1293 (2010)